ISSN 1027-4510, Journal of Surface Investigation: X-ray, Synchrotron and Neutron Techniques, 2018, Vol. 12, No. 5, pp. 944–952. © Pleiades Publishing, Ltd., 2018.
Original Russian Text © N.N. Salashchenko, N.I. Chkhalo, N.A. Dyuzhev, 2018, published in Poverkhnost', 2018, No. 10, pp. 10–20.

Maskless X-Ray Lithography Based on Microoptical Electromechanical Systems and Microfocus X-Ray Tubes

N. N. Salashchenko[a], N. I. Chkhalo[a, *], and N. A. Dyuzhev[b]

[a]Institute for Physics of Microstructures, Russian Academy of Sciences, Nizhny Novgorod, 603950 Russia
[b]National Research University of Electronic Technology MIET, Moscow, 124498 Russia
**e-mail: chkhalo@ipmras.ru*

Received January 18, 2018

Abstract—The main advantages and problems of maskless X-ray lithography (MXRL) are discussed. Consideration is given to two concepts of lithography in which the chip of a microoptical electromechanical system (MOEMS) of micromirrors and a microfocus X-ray tube chip with a “breakthrough” thin-film target are used as dynamic masks. Each of them can occupy its own niche in a research area or in the mass production of microchips. A description of the project of a MXRL facility (demonstrator of technologies), which is based on the concept of MOEMS, developed at the Institute for Physics of Microstructures, Russian Academy of Sciences, is presented for the first time.

Keywords: maskless lithography, microoptical electromechanical system, laser-produced plasma, field-emission nanocathodes, X-ray optics, multilayer mirrors

DOI: 10.1134/S1027451018050324

INTRODUCTION

Projection photolithography is a key technology of microelectronics and nanoelectronics, which specifies the limiting topological norms of microchips. The most advanced norms are achieved if immersion photolithography is employed at a wavelength of 193 nm. Modern projection nanolithography already exceeds the diffraction limit of resolution by an order of magnitude. The 10-nm half-pitch (hp) resolution, which is already a reality of mass production, is more than an order of magnitude less than the lithography wavelength [1]. Therefore, 193-nm lithography can be ranked as the top level of high technologies. Its operation implies a very developed infrastructure: equipment, methods, and technologies. The most complex and expensive components of the given infrastructure are masks. The set of masks used to produce a single chip can cost up to several million dollars. Hence, due to the high cost of equipment, high prices of masks, and complex and expensive infrastructure, projection photolithography has become competitive only under the condition of mass production. In other words, this technology requires a global market. As a whole, all of this makes the given technology viable only for individual multinational players (Intel, Samsung, TSMC, Global Foundries).

As a consequence, the technology is not flexible, forcing electronics manufacturers to orient their developments to the mass production of microelectronics even to the detriment of the performance characteristics of the product being created.

In recent years, a noticeable role has been played by 13.5-nm lithography (extreme UV (EUV) lithography). During experimental operation, this technology has been employed to fabricate the critical layers of chips [2]. The smaller operating wavelength makes it possible to decrease the number of operations during chip manufacturing, thereby decreasing the cost of the lithography process, and obtain a hp value of less than 10 nm. However, a lithograph cost of about $100 million, mask prices, and the complex infrastructure even exceed the requirements to 193-nm lithography.

Hence, the search for new nanolithography tools is very urgent. A hypothetical nanolithograph must ensure topological norms similar to those of projection lithography in the range of 100–10 nm or less. The productivity of such a nanolithograph can be one–three orders of magnitude smaller than that of projection lithography, but, undoubtedly, there must be no masks. The cost of the lithography process must weakly depend on the scale of production. It is important in principle that the lithograph cost be comparable with that of the industrial single-beam electronic lithographer. In this case, it can be said that nanoelectronic device manufacture will become attainable not only for individual multinational companies but also for smaller companies. This is critically important for Russia.

"Maskless" lithography methods incorporate electronic, ionic, optical, and different probing methods of surface modification. All of them are similar to each other in that the topology formed on a substrate is defined by software and, at any instant, can be corrected by simple changes in the algorithms of scanning by electron/light beams and probes and via other approaches. The aforementioned methods were described in several reviews, e.g., in [3, 4].

It is evident that electron-beam lithography is the most universal and advanced method. The given technology satisfies almost all requirements imposed on the above-described hypothetical lithograph except for a decrease in the productivity by six–seven orders of magnitude when the topology decreases from the micrometer to nanometer level [3]. The greatest possibilities are related to multiple-electron-beam lithography. Due to a small wavelength and even relatively slow electrons, this technology potentially ensures the fundamental resolution limit at a level of 1 nm. The main problem of electron-beam lithography is the electro-magnetostatic interaction between nanobeams leading to image blurring. Although multiple-electron-beam lithography has being studied for decades, the problem remains unsolved. In particular, the best results were obtained by Mapper Technology Co. The latest-generation setup operates with 65000 beams and maintains technological norms corresponding to 28 nm. The elementary-beam size is 25 nm, and the productivity reaches 4 wafer/h [5, 6]. The authors faced the challenge of the strong heating of wafers, and, consequently, limits on the resolution and alignment accuracy. Hence, a decrease in topological norms and an increase in productivity require further development efforts. However, in the case of success, the predicted cost of the lithograph is $100 million dollars, i.e., the given technology will be available only for global companies.

In this work, an alternative to multiple-electron-beam lithography, namely, 13.5-nm maskless X-ray lithography (MXRL), which was first proposed in [7], is discussed. The advantages and problems of the given lithography are examined. Two MXRL projects, which are being developed with our participation and are at different stages of readiness, are first reported.

MASKLESS X-RAY LITHOGRAPHY BASED ON MICROOPTICAL ELECTROMECHANICAL SYSTEM OF MICROMIRRORS

The scheme of a lithograph with a wavelength of 13.5 nm for the EUV range, in which a microoptical electromechanical system (MOEMS) of micromirrors plays the role of a photomask, was first proposed in [7]. In this technology, the topology is encoded by the state of MOEMS pixels (micromirrors) reflecting X-rays. In essence, this technology is a complete analog of multiple-beam optical lithography [8], in which refractive optics is replaced with reflecting optics. As in optical lithography, a dynamic mask is stationary, and a resist-covered wafer is scanned along two coordinates. Since the wavelength is shorter, the diffraction limit of resolution enters the nanometer region.

It can be asserted that the proposed technology is potentially a breakthrough. In particular, it was demonstrated [9] that, due to a two-coordinate scanning system and a small number of mirrors in the optical scheme, the MXRL setup ensures a productivity of the lithography process comparable with that of projection EUV lithography. However, the number of publications devoted to the given topic is extremely small. The current state of affairs can be characterized as follows. It was theoretically found that MXRL enables us to generate images with a spatial resolution defined by the focusing spot (pixel) size normalized to the reduction coefficient of the optical system under the conditions of a limited MOEMS speed, the use of a pulsed radiation source, and mechanical scanning of a photoresist-covered wafer [10–13]. The main problem impeding practical implementation of the given idea is the lack of MOEMS capable of efficiently reflecting X-rays.

Interest in the given technology has again been aroused due to the demonstration of Mo/Si multilayer mirror deposition on a commercial MOEMS with a reflection coefficient of 40% (the witness reflection was 67%) [14]. These results indicate the principle possibility of creating the key component of a maskless X-ray lithograph, i.e., a dynamic mask.

In accordance with scientific-technological data in the field of the fabrication and metrology of imaging X-ray optics with diffraction quality and those obtained both in the development of a 13.5-nm EUV lithography prototype and in the area of laser-plasma X-ray sources, which were accumulated by specialists of the Institute for Physics of Microstructures (IPM), Russian Academy of Sciences (RAS), and the potential of Belarussian Planar Co., which is the only lithography equipment manufacturer in post-Soviet territory, the project of a maskless X-ray lithograph based on a MOEMS has been developed. The goals of the project are to develop critical MXRL technologies for technological norms of 65-32/28-22-16/14 nm and create a prototype of a maskless X-ray lithograph (demonstrator of technologies).

The project's relevance is associated with the problems facing Russia, in particular, the need for a quick solution to the problem of the creation of a domestic technological base for IC production according to the technological norms of 65-32/28-22-16/14 nm with the prospect of 7 nm. From the scientific viewpoint, this is the development of innovative solutions in the field of nanolithography satisfying modern trends: equipment accessibility, low cost of utilization, and low dependence of the cost of the lithography process on the scale of production.

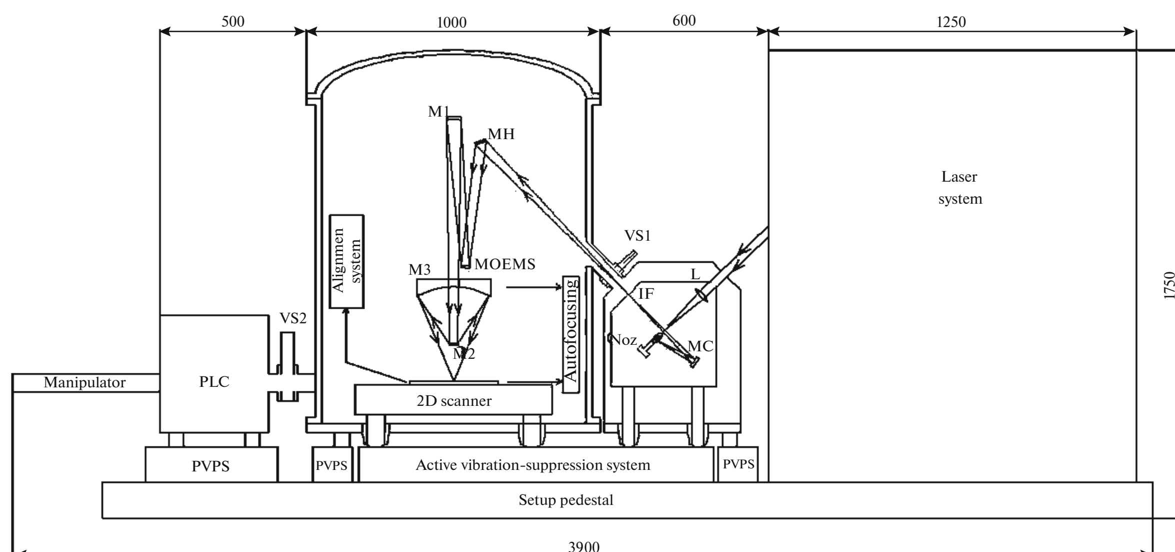

Fig. 1. Schematic representation of the MXRL setup (demonstrator of technologies) based on the MOEMS: L is the lens; Noz is the gas nozzle; MC is the mirror collector; MH is the mirror homogenizer; M1, M2, and M3 are the projection-lens mirrors; IF is the intermediate focus; MOEMS is the microelectromechanical system consisting of micromirrors; PVPS is the passive vibration-protection system; VS1 and VS2 are the vacuum valves separating the exposure chamber from the radiation source and the wafer lock chamber (PLC). The sizes are shown in millimeters.

Description of the Maskless X-Ray Lithograph (Demonstrator of Technologies)

Figure 1 provides a schematic representation of the X-ray lithograph (demonstrator of technologies). The basic systems of the setup are a vacuum chamber where resist-covered plates are exposed, a laser-plasma source of soft X-rays, a solid-state laser, a dynamic-mask illumination system, alignment and autofocusing systems, a two-coordinate wafer scanner, a lock chamber used to insert and remove exposed wafers, and active and passive vibration-protection systems. The approximate overall sizes are expressed in millimeters in Fig. 1.

The setup operates as follows. Laser radiation (pulse duration is 3–5 ns, pulse energy is 0.3–0.5 J, and the repetition frequency is 1–3 kHz) is focused by means of lens L on the gas-jet axis at a distance of 1 mm from the end of the gas nozzle Noz. In this case, a xenon gas jet is chosen. Due to gas breakdown and electron heating in the laser-radiation field, high-temperature plasma is formed. Plasma-generated Xe^{10+}–Xe^{13+} ions intensely radiate in a relatively narrow (about 0.5 nm) spectral range with a radiation peak at a wavelength of 10.8 nm.

This radiation is reflected from a mirror collimator (MC) and redirected toward a mirror homogenizer (MH). By analogy with [15], the composite MH ensures homogenous illumination of the dynamic mask (MOEMS). Upon reflection from the MOEMS, radiation impinges on mirror 1 (M1) of the projection lens. Afterward, the image is transmitted to a photoresist-covered wafer mounted in the image plane with the help of mirrors 2 and 3 (M2 and M3). The feature of the projection scheme is that beams reflected from tilted micromirrors (this state corresponds to the non-reflecting part of the photomask) miss the input lens aperture. Thus, the micromirror state is formed by a single image pixel: “0” is a tilted micromirror, and “1” is its initial state.

Only a small part of the wafer is illuminated at the laser-pulse instant. The required wafer topology is formed if the coordinated motion of the scanner and MOEMS micromirrors is synchronized with laser pulses. It is important to note that, at least in the exposed area of the wafer, its motion occurs at a constant velocity.

The system of alignment of microcircuit layers ensures accurate determination of the wafer coordinates according to markers and, during scanning, control and correction of the coordinates with the required accuracy. The autofocusing system monitors and corrects the distance between the lens and resist-covered plate with an accuracy better than the depth of the lens focus. The insertion of photoresist-covered wafers and removal of exposed plates occurs through the lock chamber.

Apart from the purely binary exposure method, it is possible to implement exposure under “grey color” gradation conditions. This is achieved if the image is multiply fixed with a small shift (smaller than the size of one pixel). Such fixing is one of the procedures of “resolution improvement”. On the whole, the interaction between the three (laser, MOEMS, and scanner)

systems provides additional opportunities for optimizing the resist-illumination profile. As a result, a high resolution and low roughness of the line edge are attained. In this respect, the optimization of the lithograph in the given system is a very interesting problem.

The project is planned to be performed in cooperation with several organizations having world-class information or the necessary competence in the chosen critical technology. In the context of cooperation, the IPM RAS, Nizhny Novgorod, is developing a setup concept, coordinating project works, developing an optical scheme and fabricating optical components and systems, depositing X-ray reflecting coatings on MOEMS, producing X-ray diagnostic systems, integrating all systems and commissioning the setup, and testing lithography processes. In this field, the Institute of Applied Physics, RAS, Nizhny Novgorod, is developing a high-power kilowatt-class laser system, a laser-plasma source of soft X-rays, and a xenon regeneration system; Riper-NN, Nizhny Novgorod, is developing X-ray resists; the Sedakov Research Institute of Measuring Systems, Nizhny Novgorod, is developing the MOEMS; the Institute of Microelectronics Technology and High Purity Materials, RAS, Chernogolovka, is developing algorithms and software of the control of lithographic processes; the Experimental Factory of Scientific Engineering, RAS, Chernogolovka, is developing a vacuum system; the Molecular Electronics Research Institute, Zelenograd, is developing plasmochemical processes of nanolithography; and Planar, Minsk, Belarus, is developing a two-coordinate scanning system, alignment and autofocusing systems, and a robot intended for wafer transport in the alignment chamber.

Description of the Key Components and Systems of the Setup

The configuration and main technical characteristics of the systems and the setup as a whole were formed considering the following.

Wavelength selection. Although the traditional wavelength is 13.5 nm, a wavelength in the neighborhood of 11 nm was chosen. It was demonstrated [16] that the given wavelength possesses the following advantages. Firstly, the projection-lens resolution exceeds 20% at the same numerical aperture (NA). For clarity, a 10-nm resolution ensured by the lens at a wavelength of 13.5 nm is scaled to 7–8 nm. Secondly, an expensive EUV source based on tin ions, which is very complex from the engineering viewpoint and requires two lasers, a high-frequency system of delivery of tin droplets, and complicated multistage systems of mirror protection against contamination with tin vapor, is replaced with a simple and “pure” source based on xenon ions. For xenon plasma, the ratio of the laser-radiation energy conversion into soft X-rays near 11 nm is 5%, i.e., corresponds to that of tin at 13.5 nm. Thirdly, since tin vapors are lacking, there is no need to purify mirror surfaces from tin with the help of hydrogen. The strong chemical activity of hydrogen imposes severe restrictions on materials used inside the setup and requires special protection of the multilayer mirrors. On account of the use of xenon, the equipment cost decreases substantially.

The final wavelength value, i.e., 11.2 or 10.8 nm, will be determined more exactly after multilayer mirrors based on yttrium and strontium and operating at 10.8 nm are studied and their efficiency is compared to that of Ru/Be multilayer mirrors with a wavelength of 11.2 nm so that the radiation spectrum of the source can be taken into account.

MOEMS selection. With the aim of the consolidation of financial, technological, and human resources, the commercially available IPMS (Dresden) MOEMS [17] fabricated according to the technology described in [18] was chosen for implementing the first stage. The pixel size was 16 × 16 μm, and the number of pixels was 1.05×10^6. In the future, its size can be decreased. In [14], a MOEMS with a pixel size of at least 8 × 8 μm was investigated. In a private conversation, those that fabricated the MOEMS assumed that a value of 4 μm could be implemented within the scope of the existing technology. In addition, there is a preliminary agreement that MOEMS production technology can be transferred to Russia.

Projection lens. This quantity is a key component defining the minimum topological norms of a lithograph. Since the specular-reflection coefficients are 70% at best, lenses of the given range are generally developed by minimizing the number of mirrors. Within the limits of the given project, it is planned that a resolution δx of better than 20 nm will be attained. In accordance with the relationship

$$\delta x = 0.61\lambda/\mathrm{NA}, \qquad (1)$$

where λ is the wavelength, the numerical aperture required to obtain the specified resolution corresponding to a wavelength of 11 nm is NA ≈ 0.34. To demonstrate that a lithography resolution of up to 10 nm can be attained without a change in the projection lens, NA = 0.4 was chosen in the project.

Figure 2 presents the optical scheme of a three-mirror lens with NA = 0.4. It is seen from Fig. 2 that 10-nm hp resolution is achieved with the same lens. In this case, it is necessary to employ a MOEMS with a pixel size of 8 × 8 μm. However, HP = 7 nm can be reached only with a lens whose numerical aperture is NA = 0.5.

Since the micromirror (pixel) size was 16 μm, ×800 lens magnification was chosen. In optimizing the geometric sizes of the optical scheme and the mirror surface shape, an additional condition was to preserve the resolution in the field of view equal to a MOEMS size of 8 × 33 mm. Optical calculations were carried out using the ZEMAX program.

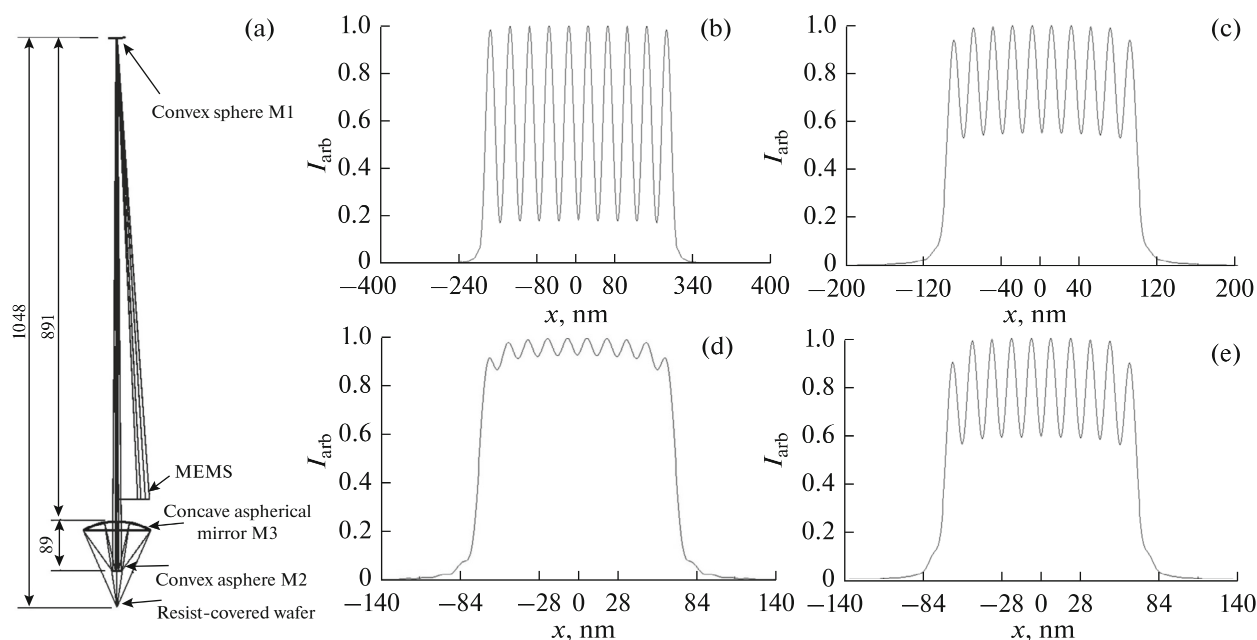

Fig. 2. Three-mirror lens with NA = 0.4: (a) optical scheme (sizes are shown in millimeters), (b) calculated band image with width hp = 20 nm at a MOEMS mirror size of 16 × 16 μm, (c) hp = 10 nm at 8 × 8 μm, (d) hp = 7 nm at 4 × 4 μm, and (e) hp = 7 nm at 4 × 4 μm and NA = 0.5.

The main parameters of the X-ray optical scheme of the objective lens and mirrors will be defined more accurately during scheme optimization, in particular, it is quite possible that an off-axis arrangement of the objective lens will be chosen in the end. However, from the presented model scheme, it can be said that mirror M1 is a simple convex sphere, while M2 and M3 are convex and concave aspherical mirrors. To achieve the required resolution and a relative large field of view, the asphere profile with respect to the parameter of deviation from the optical axis is described by a polynomial of up to eighth degree, and the maximum deviation from the nearest sphere is 4.2 μm. Production and metrology methods, which were developed at the IPM RAS, make it possible to produce such an asphere [19–21].

X-ray radiation source. At present, 13.5-nm EUV lithography employs a laser-plasma radiation source based on tin ions [22]. This source is a complicated engineering device involving a pulsed solid-state laser used to evaporate tin targets, a high-power CO_2 laser intended for plasma heating to a temperature ensuring the optimal conditions of tin-ion generation in the vicinity of 13.5 nm, and a complex high-frequency system of delivery of tin droplets. Apart from the complexity of the source itself, its use in the lithograph requires the creation of an additional infrastructure involving optics protection, first and foremost an EUV radiation collector, against tin droplets and its vapors and energetic ions. One of the most serious consequences is that the chamber constantly contains a certain amount of hydrogen. This is an additional factor limiting the use of constructional materials, including optical components.

As was indicated above, the application of such complex and expensive systems is economically justified only for global manufacturers of nanoelectronics. In the context of the given project, it is proposed to employ a laser-plasma source with a xenon-gas target. Such a radiation source was actively studied in the period from the late 1990s to the early 2000s as a candidate for 13.5-nm lithography. However, in the vicinity of 13.5 nm, the ratio of laser-radiation energy conversion into the EUV region turned out to be less than 1% for a xenon source. At the same time, its value reached 5% for tin ions. Since the radiation spectrum of xenon plasma has a peak near 11 nm [23], its shape enables us to expect a ratio of conversion at a level of 5% as well. Moreover, due to the fact that the Xe source was earlier optimized at 13.5 nm, it can be hoped that a higher conversion will be obtained. In the vicinity of 11 nm, Xe source optimization to the radiation maximum is also a problem of the project.

Requirements to the scanner and alignment system. When the basic requirements to the scanning and alignment systems were developed, it was supposed that, firstly, the scanner ensures 20-nm hp resolution and, secondly, its parameters must be compatible with the existing technological level in the production of microelectronics and nanoelectronics according to the norms of 90 nm on wafers 200 nm in diameter. This approach corresponds to the modern trend in which the main bulk of lithography on the chip is produced using a

Table 1. Main technical characteristics of the maskless X-ray lithograph (demonstrator of technologies)

Parameter	Value
Operating wavelength	11.2 nm
X-ray source size	0.3 mm
Specular-reflection coefficient	0.7
Dynamic mask type and chip and pixel sizes	MOEMS, Mo/Be M3, chip of 8 × 33 mm, pixel of 16 × 16 μm, 1.05 Mp
Objective (three lenses) NA	0.4
Reduction coefficient *M*	×800
Frame size on the wafer	10 × 41 μm
hp resolution	20 nm
Wafer diameter	200 mm
Productivity of the lithography process	2 wafer/h
Alignment accuracy	5–6 nm
Alignment accuracy in the mix-and-match mode	10–12 nm
Depth of focus	±35 nm
Maximum 2D scanner motion velocity	100 mm/s
Laser-radiation pulse frequency	≥2 kHz
Energy in each pulse	0.5 J
Pulse duration	3–9 ns
Radiation wavelength	1064 nm
Ratio of laser-radiation conversion into X-rays	0.05
Lock chamber used to insert and remove wafers	1 piece
Power consumption	25 kW
Overall sizes	3900 × 1750 × 1100 mm
X-ray resist sensitivity	0.01 J/cm^2

wavelength of 193 nm and critical layers are formed by means of EUV at a wavelength of 13.5 nm [24].

Photoresists. Within the scope of the project, it is planned that Riper-NN will renew and develop the fabrication of X-ray resists of different compositions, including those with chemical amplification developed earlier at the Research Institute for Chemistry, Lobachevsky State University of Nizhny Novgorod [25].

The main technical characteristics of the setup are summarized in Table 1. The frame size is the instantaneous image of the MOEMS. In the mix-and-match mode, the alignment accuracy implies the accuracy of alignment of topological images on the wafer upon its transport from the 193-nm lithograph to the maskless X-ray lithograph (demonstrator of technologies).

LITHOGRAPH PRODUCTIVITY ESTIMATION

The productivity of the maskless X-ray lithograph (demonstrator of technologies), the X-ray optical scheme of which is depicted in Fig. 1 and a projection-part fragment in Fig. 2, can be estimated from the following relationships.

The scheme contains six multilayer mirrors. The X-ray power P_W on a plate can be represented as

$$P_W = P_L \mathrm{CE} \frac{\Omega_{\mathrm{col}}}{2\pi} R^6 \ [\mathrm{W}], \quad (2)$$

where P_L is the laser-beam power [W], *CE* is the ratio of laser-radiation conversion into soft X-rays in the semispace, Ω_{col} is the solid angle of the collector, and *R* is the specular-reflection coefficient. Thus, the productivity of the lithography process PLP can be expressed as

$$\mathrm{PLP} = P_W / S_{\mathrm{ph}} \ [\mathrm{cm}^2/\mathrm{s}], \quad (3)$$

where S_{ph} is the X-ray resist sensitivity.

The solid angle can be approximately expressed in terms of the numerical aperture $\mathrm{NA}_{\mathrm{col}}$:

$$\Omega_{\mathrm{col}} \cong \pi \mathrm{NA}_{\mathrm{col}}^2. \quad (4)$$

The source size *s*, MOEMS size H_M, $\mathrm{NA}_{\mathrm{col}}$, and input objective-lens aperture $\mathrm{NA}_{\mathrm{in}}$ are connected by the relationships

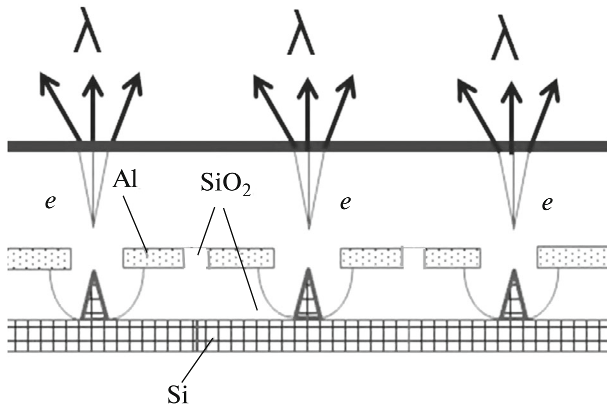

Fig. 3. Principle of operation of the MFXRT chip: *e* designates electrons and λ are X-rays formed in a thin film target.

$$\frac{NA_{\rm col}}{\rm NA_{in}} = H_M/s, \quad (5)$$

$$\rm NA_{in} \cong NA/\mathit{M}, \quad (6)$$

where NA is the numerical aperture and M is the objective-lens reduction coefficient.

When all relationships mentioned above are taken into account, expression (3) can be rewritten as

$$PLP = 1/S_{\rm ph} P_L {\rm CE} \frac{H_M^2 {\rm NA}^2}{2s^2M^2} R^6. \quad (7)$$

It follows from (7) that the productivity of the lithography process increases linearly with an increase in the resist sensitivity, laser-radiation power, the efficiency of laser-light conversion into soft X-rays, and the MOEMS area (term H_M^2) grows quadratically with increasing objective lens NA and decreasing radiation-source size; and depends on the sixth degree of the specular-reflection coefficient. Substituting the expected setup parameters from Table 1 into (7), we obtain that a productivity of a wafer 200 mm in diameter of 10.4 per hour. This estimate does not allow for a fourfold decrease in MOEMS along the second coordinate. However, due to the composite MH (taken into account in (7) by analogy with [15]) the collector's solid angle can be increased two–threefold. As a result, the losses in the MOEMS area are compensated. Thus, with the use of a laser whose average power is measured in kilowatts, it can be expected that the productivity of the lithography process will be 2.5–5 wafers 200 mm in diameter per hour. This productivity is quite sufficient for small- or medium-scale production. It should be noted that the productivity can be increased 16-fold under the condition that the micromirror size is varied from 16 to 4 μm and the topological norm remains invariable.

LITHOGRAPHY BASED ON A CHIP OF MICROFOCUS X-RAY TUBES

Lithography based on a chip of microfocus X-ray tubes (MFXRT) proposed in [26] is an alternative to the above-described MXRL based on the MOEMS and the laser-plasma source of soft X-rays. Its idea relies on the developed technology of the fabrication of pointed field-emission silicon cathodes with a control grid. The principle of operation of the MFXRT chip is illustrated in Fig. 3.

A voltage positive with respect to the pointed cathode is applied to the target. The characteristic values are 0.5–3 kV. Simultaneously, control electrodes (designated by Al) are supplied with a negative blocking voltage preventing field emission. When the blocking voltage is removed, a microbeam of electrons incident onto the target appears. X-rays are generated in the target. Since the target is thin, the absorption depth is tens or hundreds of nanometers [27] in the soft X-ray range. When the target is located close to the cathode, the microbeam size on the target and, accordingly, the X-ray pixel size can reach tens or hundreds of nanometers. Thus, a matrix source of soft X-rays is formed, the pixel state of which can be controlled by a computer.

In the given scheme, dynamic-mask and soft X-ray source functions are combined in a single device. Hence, the nanolithograph scheme is appreciably simplified (Fig. 4). The remaining devices are the chip, the two-mirror objective lens, and the resist-covered plate on the 2D scanner. Practical implementation also requires alignment and autofocusing systems.

In estimating the productivity of the lithography process, formula (7) is simplified:

$$PLP = 1/S_{\rm ph} P_e {\rm CE} \frac{{\rm NA}^2}{2M^2} R^2, \quad (8)$$

where P_e is the electron-beam power.

Table 2 presents the main parameters of the model setup used to estimate the productivity. The beam power was chosen from the condition that such a matrix ensures an average current density of 1 A/cm^2 [28] corresponding to a power of 1 kW at a voltage of 1 kV. The conversion efficiency (CE) was calculated in [29]. The productivity was PLP = 75.6 cm^2/h or 0.96 of a wafer 100 mm in size per hour. This productivity is an order of magnitude less than that of the MOEMS-based lithograph. However, its value is quite sufficient for practical applications.

The main reserve of the increase in productivity is a decrease in the radiation microbeam (pixel) size. In this case, the required increase decreases quadratically. In addition, it is possible to increase the chip size and, accordingly, the electron-beam power.

In EUV projection lithography, a serious problem is a further decrease in the wavelength. As was

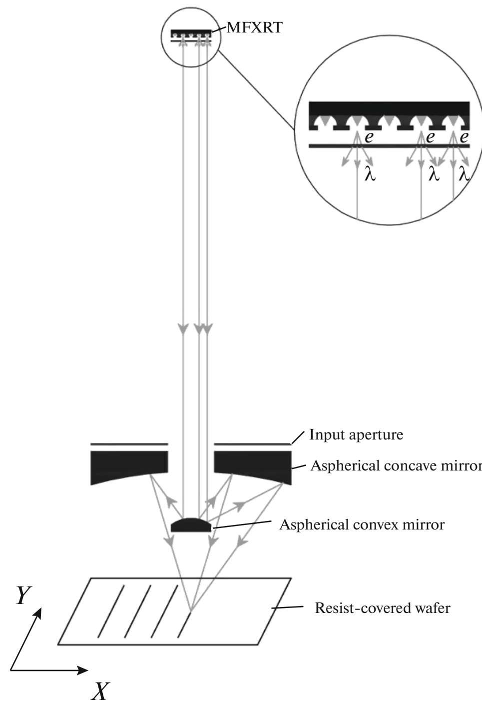

Fig. 4. X-ray optical scheme of the X-ray lithograph based on a MFXRT chip.

revealed, e.g., in [16], the peak and integral specular-reflection coefficients reduce toward the short-wavelength region. Taking into account 11–12 reflections in the scheme, such a situation becomes catastrophic. Moreover, the CE of a laser-plasma source decreases several fold, e.g., from 5% corresponding to a wavelength of 13.5 nm to 1.2–1.5% at a wavelength of 6.7 nm [30]. In the case of X-ray tubes, the CE increases with decreasing wavelength. This is caused by the fact that the probability of the radiative decay of an excited state grows with increasing energy of the given state. For example, this probability is $\omega_{Be} = 3.6 \times 10^{-4}$ for the BeK_α line ($\lambda = 11.4$ nm) and $\omega_C = 2.8 \times 10^{-3}$ for the CK_α line ($\lambda = 4.47$ nm), i.e., its value increases by an order of magnitude. Such an increase in CE can compensate a decrease in the specular-reflection coefficient. In other words, the resolution can be substantially improved if the productivity is maintained.

Table 2. Main parameters of the model setup based on the MFXRT chip

Parameter	Value
Operating wavelength	11.4 nm (BeK_α line)
X-ray microbeam (pixel) size	200 nm
Specular-reflection coefficient	0.7
Objective (two lenses) NA	0.5
Reduction coefficient M	×10
Frame size on the wafer	1 × 1 mm
hp resolution	20 nm
Electron-beam power	1 kW
Chip size	10 × 10 mm
CE	1.8×10^{-4}
X-ray resist sensitivity	0.01 J/cm^2

At the end of 2017, practical investigations into lithography mentioned above began within the scope of the applied research and exploratory development program "Development of Soft X-Ray Source Based on MFXRT for a Maskless Lithograph with a Resolution of 10 nm", (by order of the Ministry of Education and Science of the Russian Federation). The goals of the investigations were to develop a prototype of a soft X-Ray source based on a MFXRT matrix, verify experimental techniques for studying the spatial characteristics of the given type of X-Ray source, and demonstrate that the given technology is applicable to nanolithography.

DISCUSSION OF RESULTS AND CONCLUSIONS

In this work, maskless X-ray lithography, which is an alternative to multiple-electron-beam lithography, is discussed. Two types of lithography are investigated. The first of them, which was proposed in 1999 and has not yet been implemented, is based on microoptical-electromechanical-system mirrors. The second is lithography on the basis of a chip of microfocus X-ray tubes, which we proposed in 2017. By the examples of model schemes, which can be implemented in practice, the potential of the given methods, as well as niches for their application in a research area or in mass production, is demonstrated.

It is necessary to understand that the technical characteristics of the setups summarized in Tables 1 and 2 are not final. In the creation of experimental lithographs, they can turn out to be better or worse. For accurate engineering calculations, it is necessary to carry out research efforts, which have not been undertaken previously. The tabular parameters were obtained by analyzing our uncoordinated experimental data and scientific-technical publications. However, they well characterize the potential of the method and clarify the target indices.

The main outcomes of this work can be formulated as follows.

MXRL is a breakthrough technology involving a high productivity comparable with that of projection lithography and a spatial resolution and technological flexibility ensured by electron lithography. Due to considerable simplification of the X-ray source and the entire infrastructure need for its operation in lithographs and a decrease in the number of mirrors, overall sizes, and energy consumption, the setup is cheaper

by an order of magnitude as compared to a projection nanolithography setup. The absence of masks drastically reduces the cost of the lithography process and its dependence on production volumes. This technology of nanolithography is accessible not only for global players but also for smaller ones, including research companies. MXRL is ideally suitable for the Russian economy (restricted access to the world market, industry concentration on the manufacturing of unique products first of all for the military-industrial complex, and supercomputers).

The implementability of the given new lithography methods is confirmed by several significant experimental results. In particular, the theorem of existence of the MOEMS reflecting into the extreme UV range is proved. Upon solving problems concerning the creation of radiation-resistant electronics, microcircuits with large arrays of triodes, analogs of the cathode units of MFXRT, have been developed. In addition, it should be noted that almost all infrastructure created for 13.5-nm EUV lithography satisfies MXRL requirements. There are also world-class resources in Russia to solve the problems of the development of domestic MXRL equipment.

The proposed scheme of the lithographs with MFXRT is of great interest. Confirmation of the fundamental principles underlying its structure will enable us to obtain a principally new breakthrough product. Firstly, the accessibility of nanolithography increases abruptly. Secondly, there is the possibility of employing shorter wavelengths for lithography and, consequently, reaching nanometer resolutions.

ACKNOWLEDGMENTS

We are grateful to specialists of the Molecular Electronics Research Institute, namely, Academician G.Ya. Krasnikov, D. Eng. E. S. Gornev, and Cand. Sci. (Phys.–Math.) O. P. Gushchin, for numerous and valuable comments to both projects,

The work was performed using equipment of the Collective Use Center “Microsystem Technology and Electronic Circuitry” of the National Research University of Electronic Technology and supported by the Ministry of Education and Science of the Russian Federation under agreement no. 14.578.21.0250 (RFMEFI57817X0250).

REFERENCES

1. S. Jones, TSMC’s 10 nm Process Offers the Highest Transistor Density. 2018. https://seekingalpha.com/article/4151376-tsmc-intel-lead-semiconductor-processes.
2. S.-S. Kim, R. Chalykh, H. Kim, et al., Proc. SPIE **10143**, 1014306 (2017). doi 10.1117/12.2264043
3. R. Menon, A. Patel, D. Gil, and H. I. Smith, Mater. Today **8** (2), 26 (2005).
4. G. V. Belokopytov and Yu. V. Ryzhikova, Russ. Microelectron. **40** (6), 414 (2011).
5. https://www.mapper.nl/.
6. I. Servin, N. A. Thiam, P. Pimenta-Barros, et al., Proc. SPIE **9423**, 94231C (2015).
7. N. Choksi, D. S. Pickard, M. McCord, et al., J. Vac. Sci. Technol., B: Microelectron. Nanometer Struct.–Process., Meas., Phenom. **17**, 3047 (1999).
8. R. Menon, A. Patel, and H. I. Smith, Proc. SPIE **5721**, 53 (2005).
9. N. I. Chkhalo, V. N. Polkovnikov, N. N. Salashchenko, and M. N. Toropov, Proc. SPIE **10224**, 102241O1 (2016).
10. Y. A. Shroff, Y. Chen, and W. G. Oldham, Proc. SPIE **5374**, 637 (2004).
11. Y. Chen and Y. Shroff, Proc. SPIE **6151**, 61512D (2006).
12. Y. Chen, Proc. SPIE **8323**, 83231Q1 (2012).
13. K. C. Johnson, J. Vac. Sci. Technol., B: Nanotechnol. Microelectron.: Mater., Process., Meas., Phenom. **30**, 051606 (2012). doi 10.1116/1.4752112
14. N. Chkhalo, V. Polkovnikov, N. Salashchenko, and M. Toropov, J. Vac. Sci. Technol., B: Nanotechnol. Microelectron.: Mater., Process., Meas., Phenom. **35**, 062002 (2017). doi 10.1116/1.4995369
15. D. G. Volgunov, I. G. Zabrodin, B. A. Zakalov, et al., Bull. Russ. Acad. Sci.: Phys. **75** (1), 49 (2011).
16. N. I. Chkhalo and N. N. Salashchenko, AIP Adv. **3** (8), 082130 (2013).
17. http://www.ipms.fraunhofer.de/content/dam/ipms/common/products/SLM/cbm-e.pdf.
18. U. Dauderstädt, P. Askebjer, P. Björnängen, et al., Proc. SPIE **7208**, 720804 (2009). doi 10.1117/12.810787
19. N. I. Chkhalo, I. V. Malyshev, A. E. Pestov, et al., Appl. Opt. **55** (3), 619 (2016).
20. N. I. Chkhalo, S. A. Churin, M. S. Mikhaylenko, et al., Appl. Opt. **55** (6), 1249 (2016).
21. N. I. Chkhalo, I. A. Kaskov, I. V. Malyshev, et al., Precis. Eng. **48**, 338 (2017). http://dx.doi.org/10.1016/j.precisioneng.2017.01.004
22. H. Mizoguchi, H. Nakarai, T. Abe, et al., Proc. SPIE **10450**, 104500Z (2017). doi 10.1117/12.2281129
23. U. Stamm, I. Ahmad, I. Balogh, et al., Proc. SPIE **5037**, 119 (2003).
24. O. Wood, J. Arnold, T. Brunner, et al., Proc. SPIE **8322**, 832203 (2012).
25. S. A. Bulgakova, M. M. Jons, A. E. Pestov, et al., Russ. Microelectron. **42** (3), 165 (2013).
26. N. A. Dyuzhev, G. D. Demin, T. A. Gryazneva, et al., Bull. Lebedev Phys. Inst. **45** (1), 1 (2018).
27. http://henke.lbl.gov/optical_constants/filter2.html.
28. A. Basu, M. E. Swanwick, A. A. Fomani, and L. F. Velasquez-Garcia, J. Phys. D: Appl. Phys. **48**, 225501 (2015).
29. A. A. Kochetkov, A. E. Pestov, A. Ya. Lopatin, et al., in *Proc. 22nd Int. Symposium “Nanophysics and Nanoelectronics”* (Nizhny Novgorod, 2018), Vol. 1, p. 452.
30. T. Otsuka, B. Li, C. O’Gorman, et al., Proc. SPIE **8322**, 832214 (2012).
31. M. O. Krause, J. Phys. Chem. Ref. Data **8**, 307 (1979).

Translated by S. Rodikov